ISSN 0005–1144
ATKAAF 46(3–4), 143–148 (2005)

*Karl H. Edelmoser, Felix A. Himmelstoss*

# High Efficiency DC-to-AC Power Inverter with Special DC Interface

UDK 621.314.57
IFAC 4.0.1

**Professional paper**

In case of medium voltage (several tens up to hundred volts on DC-side) solar inverter applications, a DC-to-DC converter for voltage level adaptation is required in series of the DC-to-AC inverter. This leads to a two-stage concept with accumulation of the losses. In our case a concept was chosen where the efficiency of each stage is maximized by using the best topology. The given requirements make the application of a non-isolated design imperative to avoid additional transformer losses. In this paper a 60V–120V DC (input) to 230V AC (output) / 1kW converter with minimal conversion losses is derived. A simple modification in the inverter's output section leads to a significant improvement of the losses in the inverter system. Only three additional components (two diodes and one inductor) are necessary to optimize the inverter's power stage. The topology presented here shows a remarkable improvement of the switching losses and significantly reduced EMC. It is well-suited for solar power inverter applications.

**Key words:** inverter, solar power, PWM, efficiency

## 1 INTRODUCTION

Switched mode PWM inverters are industrial standard in the field of power conversion applications. The starting point of our investigations was a solar inverter of very high efficiency operating on the European power grid (230 V). Driving stages for high dynamic actuators and small motor drives are another field of application. The proposed inverter circuit can also be used as a high quality Class-D amplifier for audio applications. In this paper a new concept is shown which increases the output signal quality to meet high power quality, and reduces the electromagnetic disturbance caused by the current peaks of the power switch diode reverse recovery. As a result the overall efficiency is improved.

The main drawback of conventional PWM-inverters (cf. Figure 1) operating from a 350 V DC-link is the wide dynamic range of the output voltage (0–320 V in our case) and the required switching frequency (for minimizing the energy storage elements and coupling filters) which leads to an expensive design and increased losses. The switching ripple in the output waveform due to the limited switching frequency also requires a complex EMC-filter.

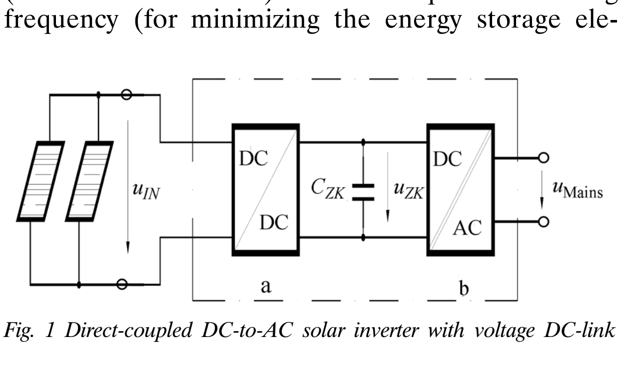


*Fig. 1 Direct-coupled DC-to-AC solar inverter with voltage DC-link*

In conventional solutions mostly standard half-bridge switching legs are used [3]. The main disadvantage of these topologies is the pronounced current peak when the opposite power switch is turned on. Due to the poor quality of the body diodes (even modern power MOSFETs contain a rather weak diode compared to usual discrete components), the switching losses of the system and electromagnetic disturbances increase. To overcome these problems, as a rule the switching speed of the power semiconductor has to be limited resulting in a further increase of the losses [4].

To overcome the known drawbacks, a topology was chosen where the inverter's power stage is discharged from switching current peaks. Separate components (power switch and diode) are used to optimize the systems behavior. So the switching speed can be increased and the required EMC-filter will be minimized. The optimized switching structure introduced in this paper leads to a more effective design. Furthermore, a very simple control scheme (similar to normal PWM operation) can be used, while the efficiency is maximized. Figure 2 depicts the converter's topology. It consists of two stages, a DC-to-DC converter (a) and a DC-to-AC inverter (b).

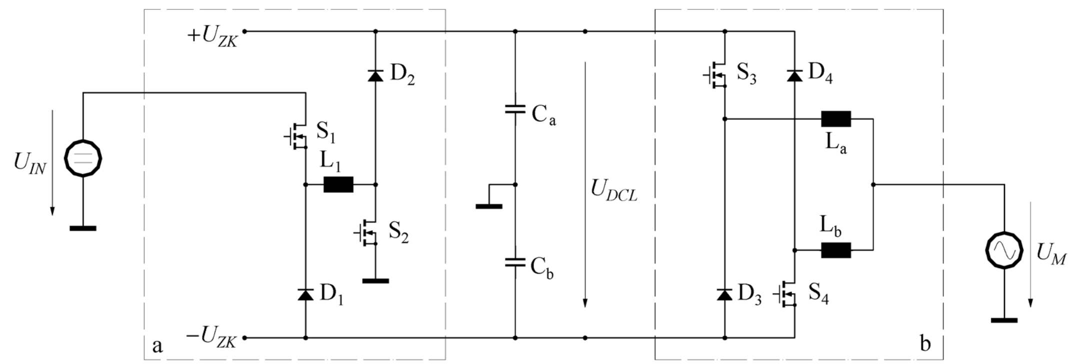


*Fig. 2 Improved power stage of the DC-to-AC inverter*

The step-up / inverting DC-to-DC converter uses an optimized structure for alternating operation. Depending on the load current polarity, normally only one direction has to be operated. During positive load current shape the step-up structure formed by $S_2$ & $D_2$ is used ($S_1$ turned on continuously). At the opposite load current direction the inverting structure formed by $S_1$ & $D_1$ is used ($S_2$ is turned on continuously). The improvement compared to standard solutions is the omission of one inductor. Furthermore, only one power switch is PWM-operated, resulting in switching losses; the second one shows only conduction losses. In the inverter stage (b) a modified half bridge structure is used. Simulation results show that the switching losses can be reduced by a factor of more than 10 compared to conventional hard switching half bridge stages, when modern components are used. The excessive current peaks in a switching leg resulting from the hard switched opposite body-diode of a power MOSFET in conventional half-bridge inverters can be avoided. The application of modern diodes (SiC) can be used here for further optimization.

## 2 DC/DC CONVERTER OPERATION

Figure 3 shows the four switching states of the proposed converter. In Figures 3.a and 3.b the step-up operation is explained, while Figures 3.c and 3.d show the step-up/down operation.

The two operating modes are used in conjunction with the inverters output voltage polarity. Depending on the output current direction, the en-

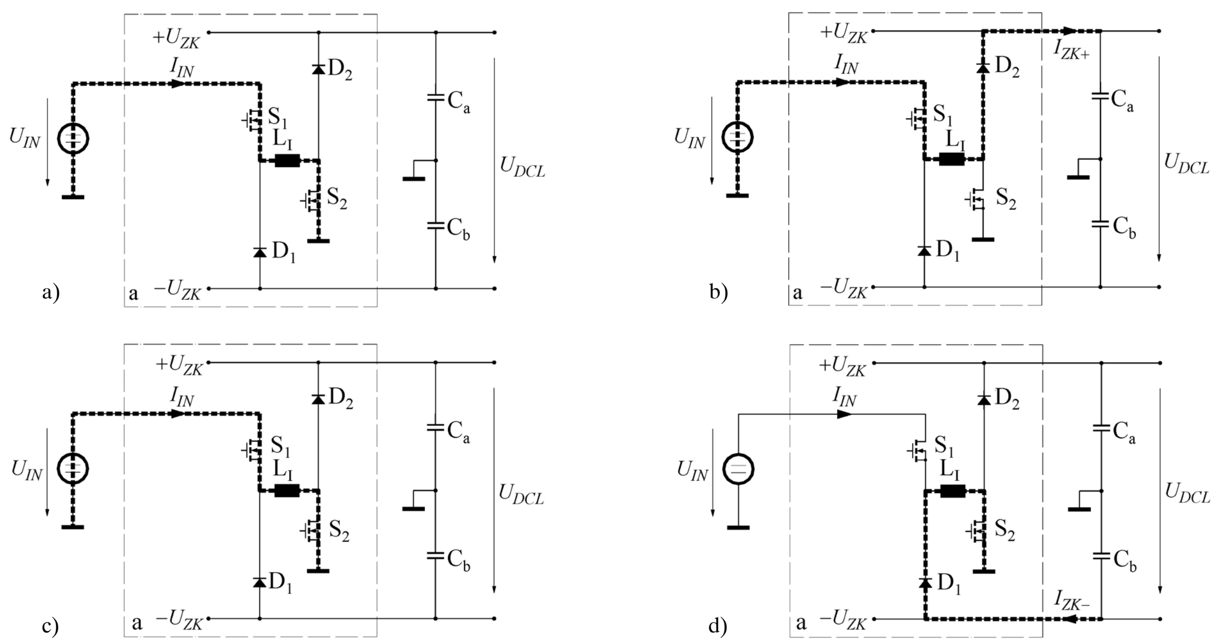


*Fig. 3 a) Operation of the step-up DC-to-DC converter (driving phase), b) Operation of the step-up DC-to-DC converter (free-wheeling phase), c) Operation of the inverting buck-boost DC-to-DC converter (driving phase), d) Operation of the inverting buck-boost DC-to-DC converter (free-wheeling phase)* ergy flow into the positive respectively negative DC-rail can be separated by an intelligent controlling algorithm leading to a minimization of the switching cycles in the DC-to-DC converter.

So a weak DC-rail (high dynamic internal resistance generated by the voltage regulator) can be used for further efficiency improvement.

With the on-time of the active switch $S_1$ $T_{ON,S1}$, the on-time of active switch $S_2$ $T_{ON,S2}$, the duty-cycle $d_1 = \frac{T_{ON,S1}}{T}$, and $d_2 = \frac{T_{ON,S2}}{T}$ the output voltages across the capacitors $C_1$ and $C_2$ for the DC/DC mode can by calculated for ideal devices and continuous inductor current mode according to

$$U_{C1} = \frac{1}{1-d_2} \cdot U_{IN} \tag{1}$$

$$U_{C2} = \frac{d_1}{1-d_1} \cdot U_{IN}. \tag{2}$$

An ideal dynamic model for the DC/DC stage with load resistors $R_1$, $R_2$ parallel to the capacitors $C_1$, $C_2$ can be given for the three stages.

At stage one the switches $S_1$ and $S_2$ are turned on

$$\frac{\mathrm{d}}{\mathrm{d}t}\begin{pmatrix} i_L \\ u_{C1} \\ u_{C2} \end{pmatrix} = \begin{bmatrix} 0 & 0 & 0 \\ 0 & -\frac{1}{RC_1} & 0 \\ 0 & 0 & -\frac{1}{RC_2} \end{bmatrix} \cdot \begin{pmatrix} i_L \\ u_{C1} \\ u_{C2} \end{pmatrix} + \begin{pmatrix} \frac{1}{L} \\ 0 \\ 0 \end{pmatrix} \cdot U_{IN}, \tag{3}$$

at stage two $S_2$ is turned off

$$\frac{\mathrm{d}}{\mathrm{d}t}\begin{pmatrix} i_L \\ u_{C1} \\ u_{C2} \end{pmatrix} = \begin{bmatrix} 0 & \frac{1}{L} & 0 \\ \frac{1}{C_1} & -\frac{1}{RC_1} & 0 \\ 0 & 0 & -\frac{1}{RC_2} \end{bmatrix} \cdot \begin{pmatrix} i_L \\ u_{C1} \\ u_{C2} \end{pmatrix} + \begin{pmatrix} \frac{1}{L} \\ 0 \\ 0 \end{pmatrix} \cdot U_{IN}, \tag{4}$$

and at stage 3 $S_1$ is turned off

$$\frac{\mathrm{d}}{\mathrm{d}t}\begin{pmatrix} i_L \\ u_{C1} \\ u_{C2} \end{pmatrix} = \begin{bmatrix} 0 & 0 & -\frac{1}{L} \\ 0 & -\frac{1}{RC_1} & 0 \\ \frac{1}{C_2} & 0 & -\frac{1}{RC_2} \end{bmatrix} \cdot \begin{pmatrix} i_L \\ u_{C1} \\ u_{C2} \end{pmatrix} + \begin{pmatrix} 0 \\ 0 \\ 0 \end{pmatrix} \cdot U_{IN}. \tag{5}$$

## 3 DC-TO-AC INVERTER OPERATION

The DC-to-AC inverter operation can also be divided into four modes depending on output polarity and switching state.

During positive output current ($I_M$) flow, the switching leg formed by $S_3$, $D_3$ and $L_c$ has to be used (Figure 4.a, Figure 4.b). Opposite to this state during the negative output current wave the second switching leg ($S_4$ $D_4$ & $L_d$) has to be used (Figure 4.c, Figure 4.d).

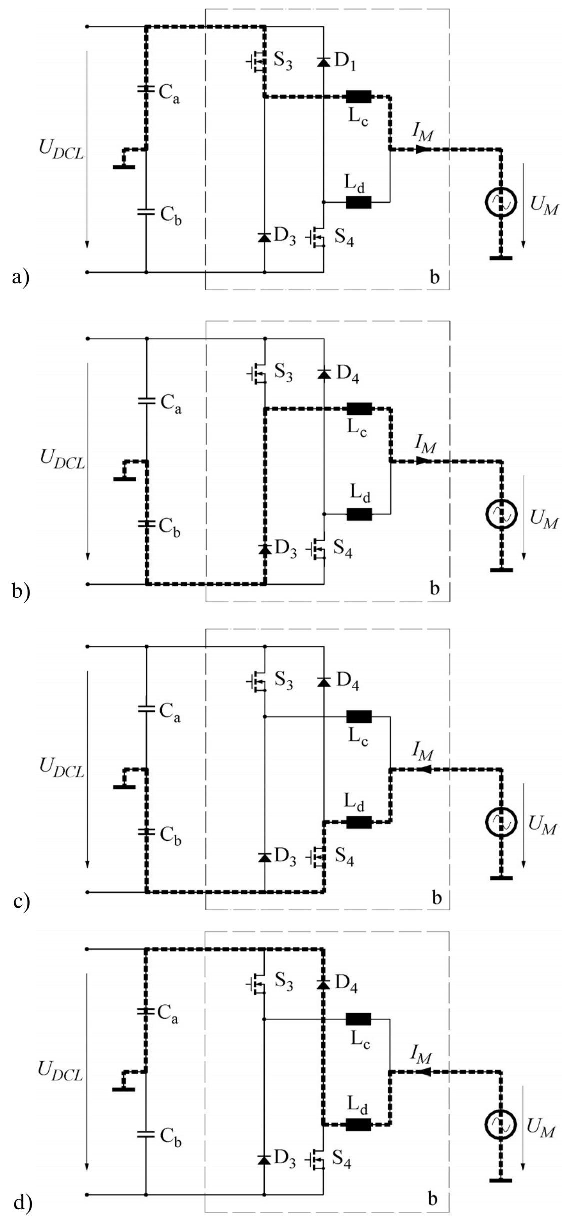

*Fig. 4 a) Operation of the DC-to-AC inverter, positive output voltage, driving phase, b) Operation of the DC-to-AC inverter, positive output voltage, free-wheeling phase, c) Operation of the DC-to-AC converter, negative output voltage, driving phase, d) Operation of the DC-to-AC converter, negative output voltage, free-wheeling phase*

The output current of the step-down stages is formed by the control law (approximation) depending on the switching states (shown for the switching formed by $S_3$, $D_3$ and $L_c$).

Driving phase ($S_3$ is turned on); duty cycle d, cycle duration

$$T: \quad 0 < d \cdot T$$

$$\frac{\mathrm{d}}{\mathrm{d}t} i_L = \frac{u_{Ca} - u_M}{L_C}. \tag{6}$$

Free-wheeling (current path through $D_3$)

$$d \cdot T < t < T$$

$$\frac{\mathrm{d}}{\mathrm{d}t} i_L = \frac{-u_{Cb} - u_M}{L_C}. \tag{7}$$

This leads to a weighted differential equation for the current

$$\frac{\mathrm{d}}{\mathrm{d}t} i_L = -\frac{u_M}{L_C} + \frac{u_{Cb}}{L_C} \cdot (2d - 1). \tag{8}$$

When the DC-link voltage and the mains voltage are known (can be measured directly), the output current of the inverter can directly be controlled by the duty-cycle of the switching stage.

The inverter's section can handle both voltage and current directions and is therefore especially well suited for local voltage generation (island applications).

## 4 DC-TO-DC CONVERTER SIMULATION

To determine the system behaviour, a circuit level based simulation (PSPICE) of the converter stage was performed. The results are shown in Figure 5 (step-up operation, ref. Figures 3.a. & 3.b.) and Figure 6 (inverting buck/boost operation, ref. Figures 3.c. & 3.d.) (converter start up).

The simulation results are compared to a conventional step-up/step-down and an isolated (transformer coupled) PWM DC-to-DC converter switching stage. Every system uses the same component models, so simulation results can be compared directly. The results are given in Table 1. As one can see, the topology used can compare favorably

Table 1 **Efficiency of the DC-to-DC converter**

| $P_{out}$ | New Top. – $\eta$ | UP/DN. – $\eta$ | Isolated – $\eta$ |
|---|---|---|---|
| 100 W | 92.4 % | 92.4 % | 85.5 % |
| 200 W | 96.1 % | 96.0 % | 94.1 % |
| 500 W | 98.5 % | 98.6 % | 96.3 % |
| 1 kW | 97.6 % | 97.9 % | 95.2 % |

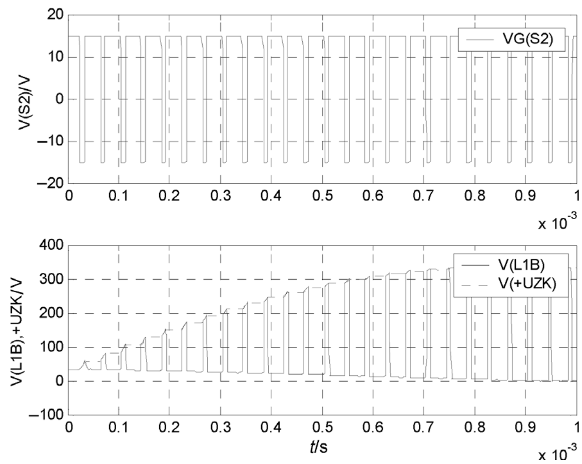


*Fig. 5 DC-to-DC converter in step-up mode*

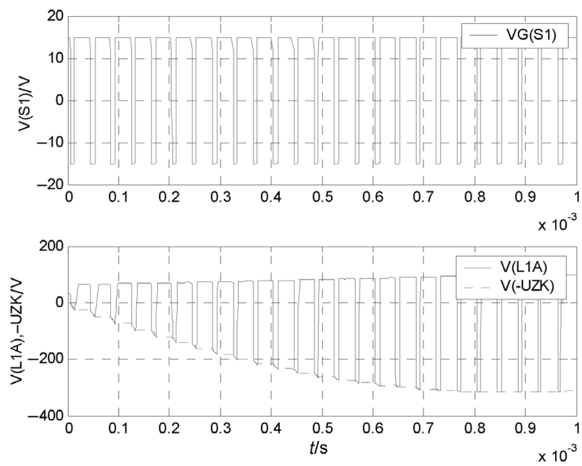


*Fig. 6 DC-to-DC converter in inverting mode*

with a conventional step-up/step-down solution. As an advantage here only one inductor is required. The simulation based on the supply of the DC-to--AC inverter stage is shown in Figure 6. (alternating current flow with mains frequency, power factor of one). The isolated topology deals with the disadvantage of the two-step energy conversion (DC-to-AC – PWM stage, transformer, AC-to-DC – rectifier, filter).

## 5 DC-TO-AC CONVERTER SIMULATION

In this section the combined inverter stage is simulated and compared to a conventional hard switched PWM stage operated at the same ambient conditions. In this model a load power factor of 1 is assumed, so the polarity of the mains current $I_M$ depends only on the polarity of the mains voltage shape. Figure 7 shows the simulation results of the power stage. In the upper trace one can see the reference current (standardized mains voltage),

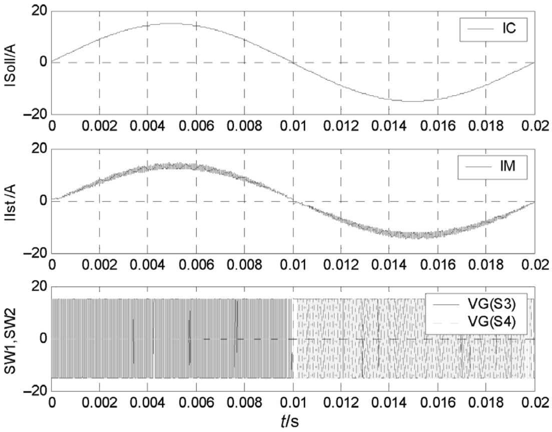


*Fig. 7 Switching behaviour of the improved inverter stage*

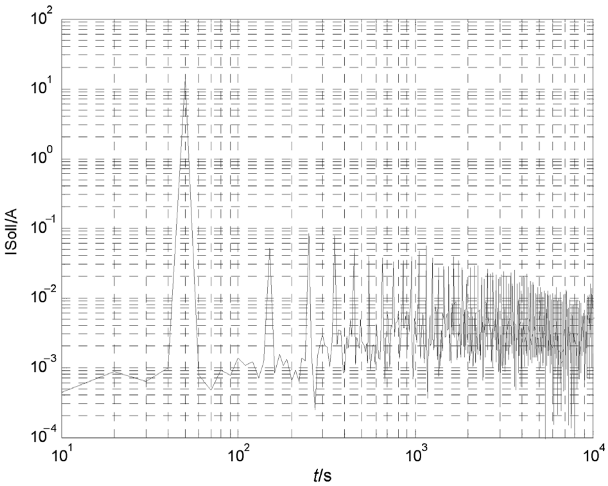


*Fig. 8 Output spectrum of the mains current, without filter*

below the resulting output current shape is shown. The lower trace shows the PWM signals of each power switch ($S_3$ respectively $S_4$).

To determine the quality of the mains current one can take a look at the output spectrum of the inverter in Figure 8. Here no additional filter is used. A simple mains coupling filter (which is always required in practical applications, but not taken into consideration here) will lead to a further improvement of the switching harmonics.

Table 2 **Efficiency conversion of the DC-to-AC inverter**

| $P_{out}$ | PWM – $\eta$ | New Top. – $\eta$ |
|---|---|---|
| 100 W | 90.5 % | 92.5 % |
| 200 W | 94.1 % | 96.1 % |
| 500 W | 96.3 % | 98.2 % |
| 1 kW | 95.2 % | 97.9 % |

The control is realized by a simple bang-bang controller and some additional logic for switching signal separation.

Table 2 compares the proposed switching stage with a conventional PWM inverter. The improvement of the advanced topology can raise the efficiency by about 2 %.

## 6 CONCLUSIONS

This new solution will reduce the disadvantage of hard-switched PWM power stages in conventional inverters. Due to the separation of the current paths, each switching leg can be optimized. Furthermore, the problem of the weak body diode can be overcome resulting in a stage with significantly lowered current peaks when modern (e.g. SiC) diodes are used.

The presented inverter stage leads to an improvement of about 2 % in over-all efficiency. This helps to simplify power inverters in the medium power range (several kilowatts).

Another advantage is the scaleable output power. The stage is best for parallel operation due to its current source characteristics. No additional external control is required.

The simple control principle of the step-down power stages can easily be implemented in a modern microcontroller without additional logic support for the pulse pattern generator. A simple PWM stage fulfils all the requirements. Also the maximum power point tracking for the solar cells can be implemented simply by monitoring the system signals ($U_{DLC}$ and $i_M$).

The new control topology can also be used to build redundant multiphase systems. The inverter presented in this paper is a simple and effective solution for medium power applications. The concept is well-suited for wind-, solar-, and renewable energy as well as aerospace applications. Because of the improved efficiency, e.g. battery lifetime can be increased without any quality reduction.

## REFERENCES

[1] P. J. Wolfs, **A Current-sourced DC-DC Converter Derived via the Duality Principle from the Half-bridge Converter.** IEEE Transactions on Industrial Electronics, Volume 40, Issue 1, Feb. 1993, pp. 139–144.

[2] V. J. Thottuvelil, G. C. Verghese, **Analysis and Control Design of Paralleled DC/DC Converters with Current Sharing.** IEEE Transactions on Power Electronics, Volume 13, Issue 4, July 1998, pp. 635–644.

[3] A. Tuladhar, H. Jin, T. Unger, K. Mauch, B. C. Burnaby, **Control of Parallel Inverters in Distributed AC Power Supply with Consideration of the Line Impedance Effect.** Applied Power Electronics Conference APEC '98, pp. 321–329, Anaheim, California.

[4] K. H. Edelmoser, **DC-to-DC Solar Power Converter for Parallel String Operation in Multi Source Structures.** Proceedings of the International Power Conversion Conference PCIM ’02, May 12–16, 2002, Nuremberg, Germany, pp. 381–386.

[5] K. H. Edelmoser, F. A. Himmelstoss, **DC-to-DC Solar Battery Converter Optimized for Parallel Operation in Multi-Source Structures.** Proceedings of the International Conference of Power and Energy Systems IASTED (Euro-PES 2002), June 25–28, 2002, Crete, Greece, pp. 406–409.

**Učinski izmjenjivač visoke djelotvornosti s posebnim istosmjernim međukrugom.** U slučajevima srednjenaponskih razina ulaznog napona (nekoliko desetaka do stotinu volti na istosmjernoj strani) izmjenjivača napajanih iz fotonaponskih ćelija, zahtjeva se istosmjerni pretvarač spojen u seriju s izmjenjivačem, za prilagodbu naponskih razina. Takav dvostupanjski pristup uzrokuje povećanje gubitaka. U ovom je slučaju odabran pristup kod kojeg se djelotvornost svakog stupnja pretvorbe maksimizira uporabom najpovoljnije topologije. Zadani zahtjevi čine obveznom uporabu istosmjernog pretvarača bez galvanskog odvajanja, da bi se izbjegli dodatni gubici u transformatoru. U ovom članku izveden je pretvarač snage 1 kW, ulaznog istosmjernog napona 60 V–120 V, izlaznog izmjeničnog napona 230 V, s minimalnim gubicima pretvorbe. Jednostavna prilagodba u izlaznom stupnju izmjenjivača dovodi do značajnog smanjenja gubitaka u izmjenjivaču. Za optimiranje izlaznog stupnja izmjenjivača potrebne su samo 3 dodatne komponente (2 diode i prigušnica). Ovdje prikazana topologija pokazuje značajno smanjenje sklopnih gubitaka i smanjuje elektromagnetske smetnje. Posebno je pogodna za primjenu kod izmjenjivača napajanih iz fotonaponskih ćelija.

**Ključne riječi:** izmjenjivač, sunčeva energija, modulacija širine impulsa, djelotvornost

**AUTHORS’ ADDRESSES**

**Dipl.-Ing. Dr. Karl H. EDELMOSER**
**University of Technology Vienna**
**Gusshausstr. 27-29- A-1040 Wien, Austria**

**Dipl.-Ing. Dr. Felix A. HIMMELSTOSS**
**University of Applied Science Technikum Wien,**
**Hoechstaedtplatz 5, A- 1200 Wien, Austria**

**E-mail: karl.edelmoser@tuwien.ac.at**
**felix.himmelstoss@technikum-wien.at**

Received: 2005-12-19